Effect of impact kinematic filters on brain strain responses in contact sports

Nan Lin, Gregory Tierney, Songbai Ji

Abstract*—*Objective: **Impact kinematics are widely employed to investigate mechanisms of traumatic brain injury (TBI). However, they are susceptible to noise and artefacts; thus, require data filtering. Few studies have focused on how data filtering affects brain strain most relevant to TBI. Here, we report that impact-induced brain strains are much less sensitive to data filtering than kinematics based on three filtering methods: CFC180, lowpass 200Hz, and a new method called Head Exposure to Acceleration Database in Sport (HEADSport).** ***Methods:*** **Using mouthguard-measured head impacts in elite rugby (N=5694), average Euclidean distances between the three filtered angular velocity profiles and their unfiltered counterparts are used to identify three groups of impacts with large variations: 90–95th, 95–99th, and >99th percentile. From each group, 20 impacts are randomly selected for simulation using the anisotropic Worcester Head Injury Model (WHIM) V1.0.** ***Results and Conclusion:*** **HEADSport and CFC180 are the most and least effective, respectively, in suppressing "unphysical artefacts" shown as sharp spikes with a rather short impulse duration (e.g., <3 ms) in angular velocity. However, maximum principal strain (MPS), especially that in the corpus callosum, is much less sensitive to data filtering compared to kinematic peaks (e.g., reduction of 3% vs. 47% and 90% for peak angular velocity and acceleration with HEADSport for impacts of >99th percentile).** ***Significance:*** **These findings confirm that the brain acts as a low-pass filter, itself, to suppress high frequency noise in impact kinematics. Therefore, brain strain can serve as a common metric for TBI biomechanical studies to maximize relevance to the injury, as it is not sensitive to kinematic filters.**

***Index Terms*—Angular velocity, brain strain, deep learning, impact kinematics, traumatic brain injury**

I. Introduction

IMPACT kinematics such as linear and angular acceleration and angular velocity have been extensively employed to characterize the severity of head impact and the risk of traumatic brain injury (TBI). In part, this is because these physical quantities can be directly measured and that they are related to tissue mechanical responses believed to cause the injury. Over the years, a wide range of instrumented sensors have become available to measure head impact kinematics [1], [2], [3]. To reconstruct head impacts on dummies in the laboratory, accelerometers and gyroscopes are instrumented at the head center of gravity to record linear acceleration and angular velocity and acceleration [4], [5]. They serve as the ground-truth to validate measurement accuracy of other impact sensors such as sensor-embedded helmets [6], in-ear sensors [7], headband for non-helmeted sports [8], skin patches [9], and instrumented mouthguard (iMG) [9], [10], [11], [12]. Once validated, these sensors are then instrumented on live humans to record impact kinematics on the field [1], [2], [7], [8], [10], [12], [13], [14], [15], [16]. They provide valuable real-world impact data to study the biomechanics of TBI, including mild TBI (mTBI) often referred to as "concussion" [1], [17].

However, noise and artefacts are common in impact kinematic measurement. As a result, signal filters are usually applied [4], [10], [11], [12], [18], [19], [20], [21], [22]. The typical approach to assessing the quality of data filtering is to compare with lab-reconstructed dummy headform impact data often regarded as the "gold standard" [18]. Most studies focus on comparing peak linear acceleration (PLA), peak angular velocity (PAV), and peak angular acceleration (PAA) magnitudes of the filtered data relative to those from lab-reconstructed or video analyzed counterparts [10], [11], [12], [20], [21].

It is important to identify the best cut-off frequency so that to minimize difference relative to signal from the gold-standard. To this end, Rowson and co-workers calculated angular acceleration from angular rate sensors and applied Channel Frequency Class (CFC) filters recommended by the Society of Automotive Engineers (SAE) J211 with different cut-off frequencies [21]. The study determined that the CFC 155 filter as the most optimal as it minimizes the root mean squared error (RMSE) relative to the 3-2-2-2 array accelerometers (normalized average error of 0.27% ± 5.2%). In comparison, Wu and colleagues compared the attenuation of filtered peak kinematics and associated injury metrics to those from high-bandwidth data to determine the best cut-off frequency [13]. It was found to be 90 Hz to maintain a 10% attenuation of PAV for helmeted dummy head impacts [12].

Other studies have also used brain strain to validate filters with lab-reconstructed reference through a finite element (FE) model of the human brain [4], [18], [22]. A physics-based brain model translates impact kinematics into detailed brain strain

Funding is provided by the National Science Foundation (NSF) under grant No. 2114697 (SJ). Impact data collection was funded by World Rugby. GT has received funding from Prevent Biometrics, Inc.

N. Lin is with the Department of Biomedical Engineering, Worcester Polytechnic Institute, Worcester, Massachusetts, USA.

G. Tierney is with School of Engineering, Ulster University, Belfast, UK.

S. Ji is with the Department of Biomedical Engineering and the Department of Mechanical Engineering, Worcester Polytechnic Institute, Worcester, Massachusetts, USA.

(Corresponding Author: S. Ji e-mail: sji@wpi.edu)

and other mechanical responses. It is considered to have strong potential to improve injury prediction and interpret kinematic exposure over global head kinematics, alone [17].

For example, Jones and colleagues investigated the feasibility of transforming current iMG system from lab tests for on-field impact measurements [18]. The study compared the 90th percentile peak maximum principal strain (MPS) of the whole brain obtained from filtered and unfiltered data. To validated the most commonly used iMG for American football head impacts, Liu and co-workers evaluated fidelity of filters using 95th percentile peak MPS of the whole brain and that of the corpus callosum, 95th percentile fiber strain in the corpus callosum, as well as several strain-related injury metrics [22]. Wu and co-workers found that the attenuation of both kinematic peaks and brain tissue responses such as strain, strain rate, Brain Injury Criteria (BrIC) and cumulative strain damage measure (CSDM) decreased when the cut-off frequency in various CFC filters increased compared to unfiltered data [13]. Work by Post et al. [23] investigated mean PLA and PAA, as well as mean MPS differences relative to the unfiltered data using various CFC filters as recommended by SAE J211 [24]. The results similarly showed that when using low-pass filters of 300 Hz or higher cut-off frequency, there were little effects on brain strain even when some difference in PLA and PAA could occur.

Nevertheless, impact kinematic filters are not consistently applied, where the cut-off frequency ranges from 100 Hz to 300 Hz, or no filter used [22], [23], [25], [26]. One study reports that PAA difference relative to the unfiltered data could range from 46% to 154% for the same signal subjecting to different filters [23]. This would lead to difficulty in assessing sensor fidelity and challenges in comparing different TBI studies for consistent findings. Given the variability in the underlying signal, a recent study suggests the need for an individualized filter based on characteristics of impact kinematic profiles instead of applying a fixed filter for all impacts [27].

To this end, a filtering method called Head Exposure to Acceleration Database in Sport (HEADSport) was developed based on the power spectral density (PSD) characteristics of reconstructed dummy head impacts and those measured on the field using the Prevent Biometrics iMGs (Minneapolis, MN) [28]. An appropriate filter frequency class was selected according to the impact kinematic PSD characteristics. Briefly, the 95th percentile of maximum PSD values from laboratory reconstructed impact signals, F_{max}, is used as a threshold. An on-field impact is considered to have artefacts, if the maximum 95th percentile PSD exceeds F_{max}. Further, frequency component above the first local PSD minima is also considered as unwanted high-frequency noise. In general, the cut-off frequency for each impact is selected as the minimum frequency among F_{max}, the 95th percentile and the first local minima (if applicable) of the PSD.

The HEADSport method was compared with two other commonly used filters, the Butterworth-200Hz low-pass (-6dB) filter used in Prevent Biometrics iMG and the CFC180 filter (-3dB lowpass, cut-off frequency of 300 Hz) that has the highest cut-off frequency in a commercially available iMG system [11]. Results showed that the HEADSport method yielded the highest signal to noise ratio (SNR). It has also been shown to be especially effective in suppressing "unphysical artefact" presented as a sharp spike in the angular velocity profile due to, e.g., mouthguard movement resulting from poor fitting, biting and direct impact to the mouthguard [28]. The sharp spike with an impulse duration <3 ms is unlikely to occur to a human head in contact sports, where an impulse duration of 10–100 ms is more typical according to reported dummy [20], [29], [30], [31], [32], [33] and on-field impacts [13], [33]. This is also consistent with the observation that angular acceleration impulse duration is typically greater than 10 ms for sports-related head impacts [34]. The artefact suppression is achieved by applying CFC filters with the lower cut-off frequency determined by its PSD, which also results in lower kinematic magnitudes relative to those from the CFC180 or 200 Hz filters [28].

In this study, we extend the comparisons of HEADSport with the same two other filters in terms of brain strain responses, including MPS of the whole brain and that of the corpus callosum deep in the brain, as well as their spatial distributions. Previous studies investigating filter effectiveness in terms of brain strains have largely focused on the peak MPS of the whole brain [4], [18], [23], with one exception comparing MPS and white matter fiber strain of the corpus callosum [22] through a deep learning neural network model [35]. The attention on brain strain deep in the parenchyma due to kinematic variations has emerged [36], [37], [38]. Because of the brain's viscoelasticity, deformation attenuation is expected when displacement travels from the brain-skull interface to the deep region. Nevertheless, the significance of impact kinematic filtering on the attenuation and the resulting deep region brain strain has not been studied. Thus, findings from this study may provide improved insight into the causal relationship between impact kinematics and brain strain. This would inform how best to maximize the utility of impact-induced brain strains for studying the biomechanical basis of TBI in the future.

II. MATERIALS AND METHODS

The HEADSport was developed based on N=5694 on-field head impacts measured by mouthguard (Prevent Biometrics; Minneapolis, MN) in elite rugby (all video-verified) and 72 lab reconstructed head impacts with various impact locations and linear acceleration magnitudes based on on-field measurements [28]. Each participant provided written consent. Ethical approval for impact data collection was given by the University's Research Ethics Committee (UREC), University of Ulster (#REC-21-0061).

Each impact had a linear acceleration profile and an angular velocity profile along the three anatomical axes prescribed at the head center of gravity. Both accelerometer and gyroscope signals have a bandwidth well in excess of 400 Hz. The measured kinematic profiles were filtered using either 200Hz, CFC180, or HEADSport, respectively [28]. Given that linear kinematics common in contact sports generate little brain strain, here we used angular kinematics, alone, for analysis [17]. All filtered or unfiltered impact kinematic profiles had a duration of 50 ms and were sampled at a frequency of 3.2 kHz. Angular

acceleration was then calculated *via* a forward differentiation method based on the angular velocity profile.

A. Euclidean distance to identify impacts for model simulation

Due to the high computational cost in impact simulation to generate brain strain (typically hours for each impact [17]), it was not feasible to simulate all the measured impacts using a conventional finite element brain model (requiring approximately six weeks to simulate and post-process just the 10% of the cases selected if run sequentially; see later for details). Thus, we limited our investigations to impacts with larger differences between filtered and unfiltered kinematic profiles. Both the peak magnitude and the shape of kinematic profile significantly affects brain strains [36], [39]. Intuitively, therefore, piece-wise Euclidean distance [40], [41] was used to quantify kinematic profile differences as this metric considers differences at every time point. Since brain strains are primarily induced by head rotation in contact sports and that brain strain is most relevant to angular velocity [36], [42], only the angular velocity profiles around the three anatomical axes were used for calculation.

The two-dimension profile matrix of data size of 160 × 3 (for a duration of 50 ms at a sampling frequency of 3.2 kHz) for each filtered and unfiltered impact was first reformatted into a one-dimensional vector (m × n = 480 × 1). It was then normalized relative to the largest component magnitude of the unfiltered data (i.e., $max(x_i)$, where i ranges from 1 to 480) to allow comparison across head impacts of different magnitudes [43]. Piece-wised Euclidean distance between each filtered and the unfiltered profile, $E(x, y)$, is then defined as below:

$$E(x,y) = \sqrt{\sum_i^m (x_i - y_i)^2} \quad (1)$$

where m is the length of the reformatted kinematics data (i.e., 480), x and y are i^{th} element in the normalized filtered and unfiltered impact profile, respectively. The resulting Euclidean distances corresponding to the three filters were finally averaged (see Fig. 1 for distribution) to characterize the degree of variation between filtered and unfiltered data.

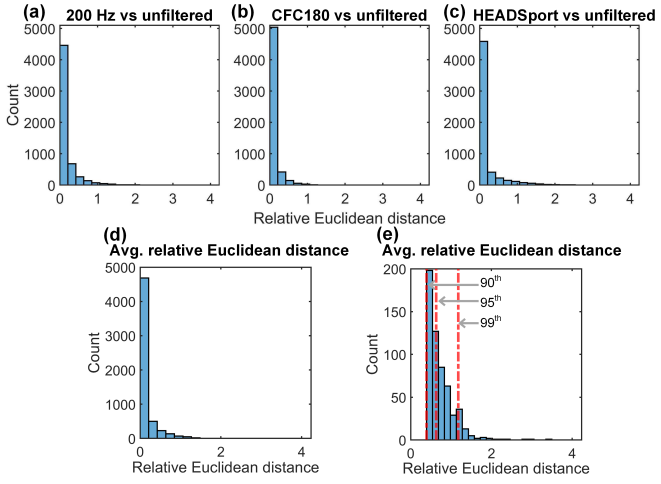

Fig. 1. Euclidean distance between filtered and the unfiltered impact angular velocity profiles for the three filtering methods (a–c) and the average Euclidean distance across filters (d). A closer view of the distribution larger than the 90th percentile of the entire dataset is shown in (e).

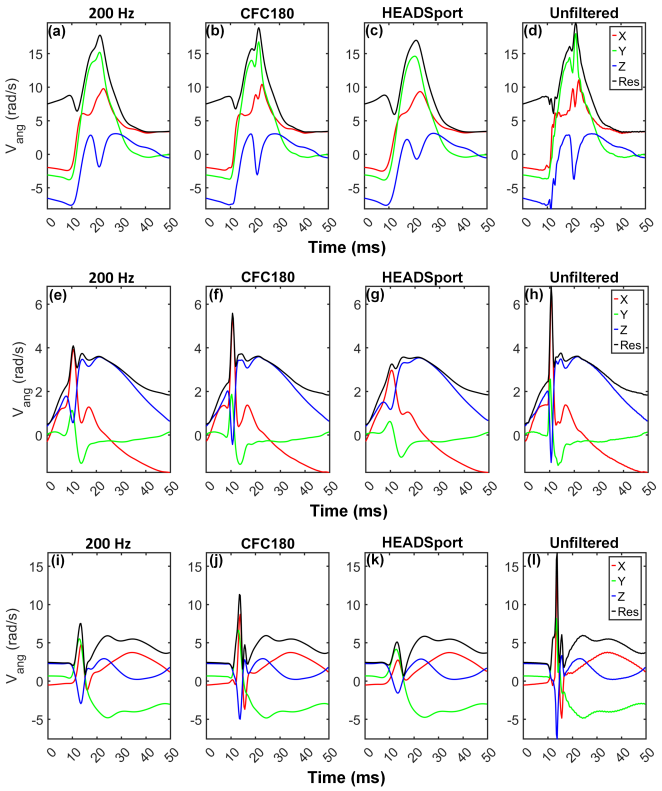

Fig. 2. Example angular velocity profiles of the three groups based on the average Euclidean distance: (top) between 90th to 95th percentiles; (middle) between 95th to 99th percentiles; and (bottom) above the 99th percentile. Both 200Hz and HEADSport are effective in suppressing the artefact shown as a sharp spike in angular velocity profiles.

B. Selection of impacts

To limit the number of impacts for model simulation, impacts with average Euclidean distances above the 90th percentile were selected for impact simulation. For a more systematic investigation, these impacts were further divided into three groups with the average Euclidean distances between the 90th and 95th, 95th and 99th, and above the 99th percentile. They had 284, 228, and 57 impact cases, respectively (Fig. 1). For each group, 20 cases were then randomly selected (sample profiles for each group are shown in Fig. 2). Next, the filtered and unfiltered angular velocity profiles for each impact were simulated using the anisotropic Worcester Head Injury Model (WHIM) V1.0 [44]. This brain model adopts hyper-viscoelastic material properties for the brain and further incorporates white matter anisotropy based on whole-brain tractography. The model has been extensively validated against relative brain-skull displacement and marker-based strain in cadaveric impacts, as well as full-field strain under *in vivo* head rotations relevant to acute brain injury and subconcussion, respectively [45]. It achieves an average peak strain magnitude ratio (simulation vs. experiment) of 0.94 ± 0.30 based on marker-based strains in 12 cadaveric impacts. A ratio of 1.00 ± 0.00 would indicate an identical peak response relative to experiment (albeit errors in experimental data, themselves,

should not be ignored [46]).

For each impact, 4 simulations (three filtered profiles plus an unfiltered profile) were conducted, leading to N=240 (20 × 3 × 4) simulations in total. After each simulation, voxelized MPS at an isotropic spatial resolution of 4 mm^3 were obtained [47]. Voxelized MPS effectively applies a median filter to mitigate concerns on numerical artefacts typically associated with the 100th percentile peak MPS [48].

C. Data analysis

The filtered and unfiltered angular velocity profiles were compared in terms of PAV and PAA resultant magnitudes. Their resulting strains were also compared using peak MPS of the whole brain and that of the corpus callosum. Percentage differences from the filtered impacts relative to those from the unfiltered impacts were reported. For MPS of the whole brain, we also reported the magnitude and distribution differences in terms of linear regression slope, k, and Pearson correlation coefficient, r. Briefly, the brain MPS of a filtered impact was considered sufficiently similar to that from the unfiltered counterpart when both k and r were within 0.1 relative to 1.0 (when the two were identical [48], [49], [50]).

Not all data samples passed the normality test. Therefore, non-parametric Mann-Whiteney U tests were conducted for group average comparisons. Linear regression models were also fit to investigate the strength of statistical association. For all statistical tests, significance level was defined at the p-value of 0.05. All head impacts were simulated using the anisotropic WHIM V1.0 [45] in Abaqus/Explicit (Version 2018; Dassault Systèmes, France). Each impact simulation of 50 ms required ~20 mins (double precision with 15 CPUs; Intel Xeon E5-2698 with 256 GB memory). All data analyses were conducted in MATLAB (R2022b; MathWorks, Natick, MA).

III. Results

Percentage differences of PAV, PAA, peak MPS of the whole brain and that of the corpus callosum from the three filtering methods relative to those from the unfiltered counterparts are reported in Figs. 3, 4, 5, and 6, respectively. For nearly all impacts, data filtering decreased response values relative to their counterparts from the unfiltered impacts, regardless of the response variable or filter used. This was especially true for PAA, as all filtered data had a substantial decrease (e.g., up to 98% for cases with the average Euclidean distance above the 99th percentile). For both PAV and PAA, the effect from HEADSport was the most evident as it led to the greatest reduction, especially PAA.

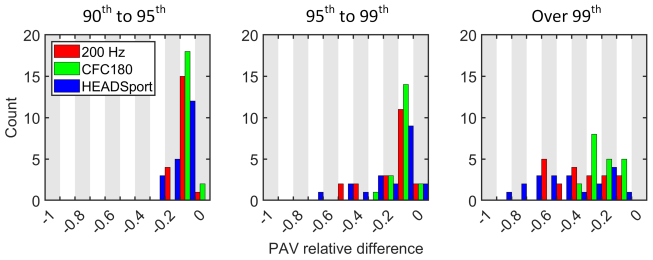

Fig. 3. Histogram number of impacts from the selected 20 cases in the three groups (from left to right) as a function of PAV percentage differences relative to those from the unfiltered data for the three filtering methods. The range of the right-most histogram bar is 0–10 %, and all relative differences are below 10% (same for Figs 4–6).

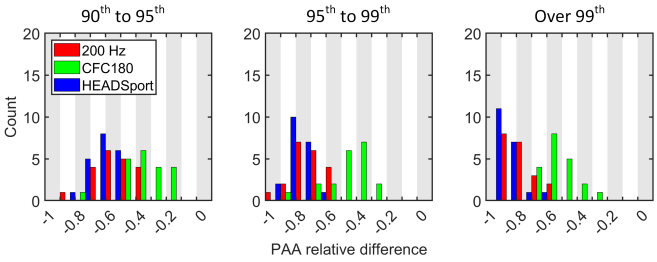

Fig. 4. Histogram number of impacts from the selected 20 cases in the three groups as a function of PAA percentage differences relative to those from the unfiltered data for the three filtering methods.

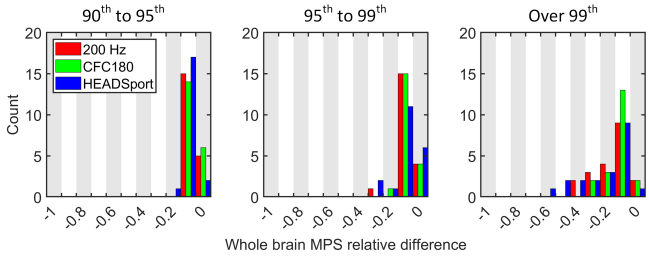

Fig. 5. Histogram number of impacts from the selected 20 cases in the three groups as a function of percentage differences of peak MPS of the whole brain relative to those from the unfiltered data for the three filtering methods.

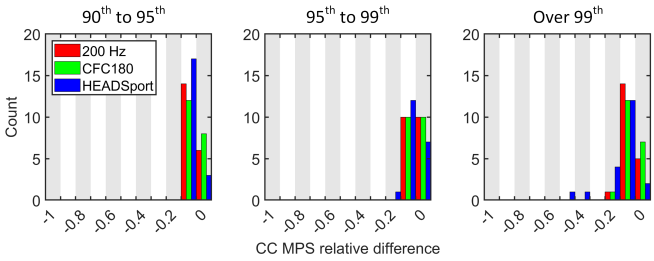

Fig. 6. Histogram number of impacts from the selected 20 cases in the three groups as a function of percentage differences of peak MPS of the corpus callosum relative to those from the unfiltered data for the three filtering methods.

However, in terms of MPS, the significance of different filters was substantially reduced. For example, for MPS of the whole brain, the filters had some substantial effect (e.g., reduction > when the average Euclidean distance was greater than the 99th percentile (Fig. 5), and the reduction was mostly within 20% for other two groups of impacts (except a few for HEADSport when the impacts were between 95th and 99th percentile). For MPS in the corpus callosum, only HEADSport had some reduction for impacts above the 95th percentile in average Euclidean distance (Fig. 6).

The removal of the artefact had a significant effect on peak kinematic magnitudes. These cases were mostly categorized as "above 99th percentile". For this category, the median relative PAV and PAA difference of HEADSport are 47% and 90%, compared to 19%/51% and 30%/77% for CFC180 and 200Hz, respectively. However, when considering peak MPS of the whole brain and in the corpus callosum, the relative differences were much reduced (p < 0.05). The median differences were 9%, 3% and 4% for peak whole brain MPS of HEADSport, CFC180, and 200Hz, compared to 3%, 0.1% and 0.5% for those

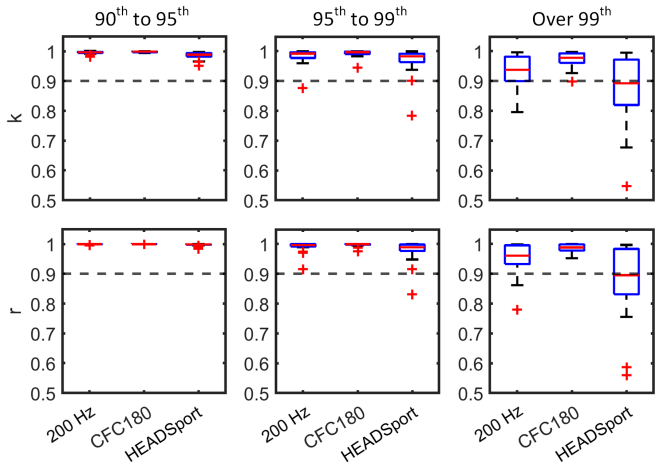

Fig. 7. Range of k (top) and r (bottom) for peak MPS magnitude and distribution for the three filtered impacts relative to the unfiltered raw data across the three impact groups. When both k and r are above 0.9 (dash-lines), the peak MPS responses are considered sufficiently similar to the counterpart from the unfiltered data.

in the corpus callosum.

To understand how MPS across the brain varied due to the use of filters, Fig. 7 reports boxplots of k and r for the three filters and the three impact groups. For most impacts with an average Euclidean distance below the 95th percentile, little effect from filters existed. For those above the 99th percentile, 200Hz and HEADSport had much more significant effect than CFC180. This was consistent with reports in Figs. 5 and 6.

Figs. 8 and 9 provide examples of MPS distributions resulting from filtered impacts and those from unfiltered data for two impacts. The MPS magnitude and distribution from filtered data were similar relative to the simulated result from the unfiltered impact for case 1 (Fig. 8; impact profiles in Fig. 2 top; average Euclidian distance 90th–95th percentile). However, they were significantly different for case 2 when using 200Hz and HEADSport as the filter (Fig. 9; impact profiles in Fig. 2 bottom; average Euclidian distance >99th percentile). Nonetheless, the MPS magnitude and distribution in the corpus callosum remained more similar in magnitude and pattern for both cases.

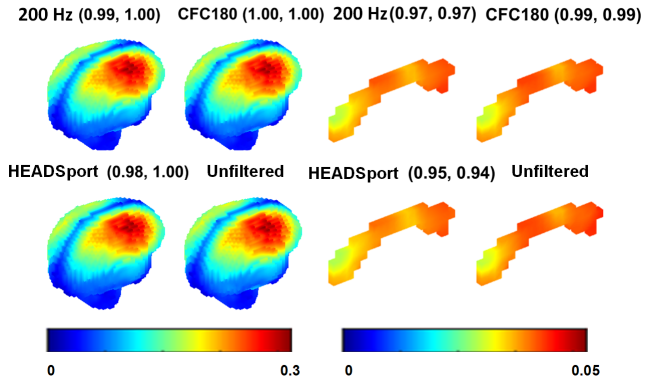

Fig. 8. An example impact case where MPS magnitude and distribution for the whole brain (left panel) and the corpus callosum (right panel) from filtered data are rather similar to those from the unfiltered data. Strains are shown in a voxelized format. Data in parentheses indicate k and r values.

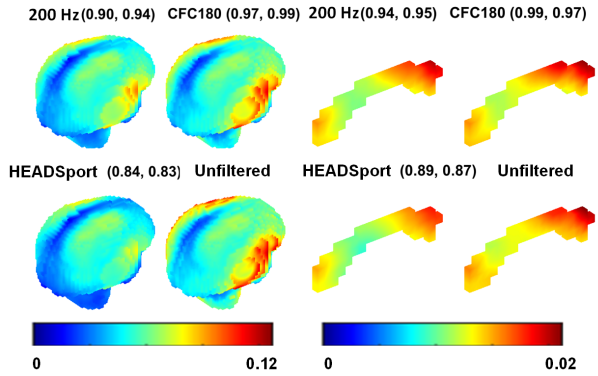

Fig. 9. An example case where larger differences in MPS magnitude and distribution for the whole brain exist (left panel), especially for 200Hz and HEADSport. However, their MPS magnitude and distribution in the corpus callosum (right panel) remain more similar.

IV. Discussion

A. *Effect of filters on brain strains*

Filter design of head impact kinematics in contact sports has been extensively studied. Nonetheless, a well-accepted and universally applicable filter or filtering method does not yet exist. A filtering method called Head Exposure to Acceleration Database in Sport (HEADSport) was recently developed based on the frequency characteristics of lab-reconstructed and measured head impact kinematics [28]. It has the potential to be more universally applicable because an appropriate individualized filter is selected for the impact under scrutiny according to the noise level and occurrence of artefact based on the power spectrum density (PSD) characteristics. Based on a subset of measured on-field head impacts in elite rugby, we found that both HEADSport and 200Hz, especially the former, were effective in suppressing artefacts that are often presented as a "sharp spike" of a rather short temporal duration (e.g., <3 ms) in the head angular velocity profiles (e.g., Fig. 2 bottom). These "spikes" do not seem physically realistic for a head impact of a live human, as they often come from unexpected movement such as biting and hitting directly to the mouthguard unrelated to head impact [28].

The removal of the artefacts had a significant effect on peak kinematic magnitudes, especially for impacts with the average Euclidian distance between filtered and unfiltered angular velocity profile above the 99th percentile (Fig. 2). For these impacts, the median relative difference for PAV and PAA were 47% and 90% for HEADSport, compared to 19%/51% and 30%/77% for CFC180 and 200Hz, respectively (Figs. 3 and 4). However, when considering peak MPS of the whole brain and that in the corpus callosum, the relative differences were much reduced. For example, the median difference for the two strains were of 9% and 3% for HEADSport, and they were 3% and 0.1% for CFC180 and 4% and 0.5% for 200Hz, respectively (Fig. 5 and 6).

These results are similar to a previous study applied to impacts in ice-hockey (e.g., average difference in PAA of 113% vs. 6.4% for MPS of the whole brain when applying a CFC filter to puck-to-head impacts with a cut-off frequency of 300 Hz)

[23]. Notably, the latter study employed a different brain injury model called the University College Dublin Brain Trauma Model (UCDBTM). To a certain degree, this suggests some consistent responses across brain injury models.

In general, relative differences for MPS of either the whole brain or those in the corpus callosum were statistically smaller than those of PAV and PAA across the impact analyzed (Figs. 3–5; $p<0.05$). Across all impacts selected for analysis, larger strain differences were strongly associated with larger differences in PAV according to a linear regression model ($p<0.05$), as expected. For example, across the three impact categories from the 90th-95th percentile to >99th percentile in average Euclidean distance, median peak MPS difference increased from <0.3% to 5%, but median PAV relative difference increased from 3% to 30%.

Similar MPS distributions (i.e., both k and r deviated from a value of 1.0 by no more than 0.1 [48], [50]) were obtained for nearly all impacts when using CFC180 and 200Hz filters, regardless of the impact category. For HEADSport, however, similar MPS distributions relative to the unfiltered data only happened for impacts within 90th-95th percentile differences, and much larger differences were found for impacts above 99th percentile (Fig. 7). Across the three filters, CFC180 consistently produced MPS distributions closest to the unfiltered data.

It should be noted that this study focused on impacts that differed the most (i.e., above 90th percentile) relative to the unfiltered data according to piece-wise Euclidean distance. Given that similar strains were obtained for nearly all impacts with the Euclidean distance between the 90th and 95th percentiles, regardless of the filters used (Figs. 8 and 9), it is expected that even closer brain strains will occur for the vast majority of impacts that had a smaller Euclidean distance (i.e., <90th percentile). Even for HEADSport, larger differences in brain strain (k or r over 0.1 far away from 1.0 [48], [50]) were observed only in impacts with the average Euclidean distance above 95th percentile (e.g., 1 out of 20 cases between 95th and 99th percentile and 60% of cases >99th percentile).

Based on these observations, it was clear that relative differences in terms of brain strains were much reduced compared to relative differences in PAV and PAA kinematics when applying filters to the angular velocity profiles. For the vast majority of impacts, there was little difference in brain strain when applying the three selected filters, unless significant artefacts occurred that appeared as sharp spikes in angular velocity profiles. For impacts with apparent artefacts, both HEADSport and 200Hz, and especially the former, were effective in suppressing the artefacts.

These findings suggest that the brain acts as a low-pass filter, itself, when subjecting to an external head impact, especially for brain strain in the deep region. A recent study reports that the temporal history of both MPS of the whole brain and fiber strain of the corpus callosum are "smoothed" relative to the input resultant angular velocity, with a cross-correlation of 0.83 and –0.52 between the two strain measures and the resultant angular velocity profile [38]. This leads to limited effect on brain strain when applying an initial low-pass filter to the impact kinematics serving as input.

B. Implications

Both PAV and PAA have been extensively employed to quantify head impact severity [1], [11], [51]. However, they could be sensitive to noise-reduction data filters that would lead to unwanted inconsistencies across studies [23]. Our findings suggest that impact-induced brain strain, particularly those in the deep brain such as in the corpus callosum, is much less sensitive to kinematic filters. Conceivably, therefore, brain strains can be used in place of PAV or PAA to quantify impact severity. They may be better positioned to serve as a common metric for comparison, which is anticipated to maximize relevance to the injury in cross-sectional and longitudinal TBI biomechanical studies, as well as across study sites.

However, a deep learning surrogate model is necessary to translate impacts into brain strains on a large-scale, as it would dramatically reduce the computational cost associated with direct model simulations while retaining a high accuracy. Several current deep learning models employ angular velocity and acceleration profiles at a temporal resolution of 1 ms as the input [35], [48], [50], [52]. The recorded head impacts are typically sampled at a higher sampling rate [11] (e.g., 3.2 kHz in this study). To use these deep learning models without re-training, impact profile down-sampling is necessary to match with the required input. This is analogous to applying a low-pass, median filter. Based on findings from this study, these deep learning models would remain valid without re-training when using down-sampled kinematic profiles as input. However, for other deep learning models that use peak values of PAV/PAA directly as input [53], this may not be feasible because their values could be significantly altered due to the down-sampling that would invalidate the predictions, especially when the signal has apparent "artefacts".

C. Limitation

This study has a few limitations. First, while HEADSport is effective in suppressing artefacts in angular velocity profiles [28], a ground-truth, nevertheless, does not exist for on-field impacts. Video-reconstructed impacts [54] may provide additional verification of the filter effectiveness for measurement of real-world head impact. Second, the number of filters considered was also limited to those analyzed in the previous study [28]. Third, we have focused on brain strain for analysis but not strain rate [55], as there is no well-accepted experimental data appropriate for strain rate validation at this stage [46].

Nevertheless, additional results on brain strain rate are reported in the Appendix. Briefly, we found that the relative differences in peak strain rate of the whole brain were larger than those for peak MPS of the whole brain in general (e.g., median difference of 71% vs. 9% for HEADSport for impacts with the average Euclidean distance above the 99th percentile). However, relative differences in peak strain rate in the corpus callosum were also smaller than those of the whole brain (e.g., median difference of 60% vs. 71% for HEADSport for impacts in the same category), which was similar to peak MPS.

V. Conclusion

For the three filtering methods studied here, we find that HEADSport and 200Hz, especially the former, are effective in suppressing unphysical artefacts in impact angular velocity profiles (e.g., sharp spikes). Nevertheless, for the majority of head impacts where no such artefacts are present, there are little differences among the three filtering methods or relative to the unfiltered data in terms of peak angular velocity magnitudes. In comparison, peak angular acceleration magnitudes could vary substantially. These findings suggest potential data inconsistencies across different TBI biomechanical studies, especially when using peak angular accelerations, if different signal filters are used. However, differences among filters and the unfiltered impacts are much reduced in their resulting brain strains, especially for strain in the deep brain such as in the corpus callosum.

There is consensus that brain strain is better positioned than impact kinematics as an injury metric for TBI biomechanics. This study finds that brain strain is not sensitive to kinematic filters due to the brain's viscoelastic nature. This makes brain strain predictions consistent regardless of the kinematic filters used. Therefore, brain strain as a common injury metric is anticipated to maximize relevance to the injury. Nevertheless, a deep learning brain injury model is necessary to rapidly translate impacts into brain strains on a large-scale while retaining a high accuracy relative to direct model simulation. This is consistent with recent consensus in the TBI biomechanics community to promote the use of advanced data science techniques, including deep learning, into future TBI studies [17]. However, caution is warranted as brain strains from different "validated" injury models may differ even when simulating the same head impact [56]. Therefore, brain strains from different models may not be compared directly.

VI. DECLARATION OF CONFLICT OF INTERESTS

The authors declare no conflict of interests.

References

[1] K. L. O'Connor *et al.*, "Head-Impact–Measurement Devices: A Systematic Review," *J. Athl. Train.*, vol. 52, no. 3, pp. 206–227, Mar. 2017, doi: 10.4085/1062-6050.52.2.05.

[2] L. Gabler *et al.*, "Consensus Head Acceleration Measurement Practices (CHAMP): Laboratory Validation of Wearable Head Kinematic Devices," *Ann. Biomed. Eng.*, vol. 50, no. 11, pp. 1356–1371, Nov. 2022, doi: 10.1007/S10439-022-03066-0/TABLES/2.

[3] D. A. Patton *et al.*, "Head Impact Sensor Studies In Sports : A Systematic Review Of Exposure Confirmation Methods," *Ann. Biomed. Eng.*, vol. 48, no. 11, pp. 2497–2507, 2020, doi: 10.1007/s10439-020-02642-6.

[4] L. C. Wu *et al.*, "Bandwidth and sample rate requirements for wearable head impact sensors," *J. Biomech.*, vol. 49, no. 13, pp. 2918–2924, 2016, doi: 10.1016/j.jbiomech.2016.07.004.

[5] N. J. Cecchi *et al.*, "Laboratory evaluation of a wearable head impact sensor for use in water polo and land sports," 2020, doi: 10.1177/1754337120901974.

[6] R. M. Greenwald *et al.*, "Head Impact Severity Measures for Evaluating Mild Traumatic Brain Injury Risk Exposure," *Neurosurgery*, vol. 62, no. 4, pp. 789–798, 2008, doi: 10.1227/01.neu.0000318162.67472.ad.Head.

[7] S. B. Sandmo *et al.*, "Evaluation of an In-Ear Sensor for Quantifying Head Impacts in Youth Soccer," *Am. J. Sports Med.*, vol. 47, no. 4, pp. 974–981, 2019, doi: 10.1177/0363546519826953.

[8] C. M. Huber *et al.*, "Laboratory assessment of a headband-mounted sensor for measurement of head impact rotational kinematics," *J. Biomech. Eng.*, vol. 143, no. 2, pp. 1–5, 2021, doi: 10.1115/1.4048574.

[9] E. E. Kieffer *et al.*, "A Two-Phased Approach to Quantifying Head Impact Sensor Accuracy: In-Laboratory and On-Field Assessments," *Ann. Biomed. Eng.*, vol. 48, no. 11, pp. 2613–2625, 2020, doi: 10.1007/s10439-020-02647-1.

[10] A. Bartsch *et al.*, "Validation of an 'Intelligent Mouthguard' Single Event Head Impact Dosimeter.," *Stapp Car Crash J.*, vol. 58, no. November, pp. 1–27, 2014.

[11] B. Jones *et al.*, "Ready for impact? A validity and feasibility study of instrumented mouthguards (iMGs)," *Br. J. Sports Med.*, vol. 56, no. 20, pp. 1171–1179, 2022, doi: 10.1136/bjsports-2022-105523.

[12] D. B. Camarillo *et al.*, "An instrumented mouthguard for measuring linear and angular head impact kinematics in American football.," *Ann. Biomed. Eng.*, vol. 41, no. 9, pp. 1939–49, Sep. 2013, doi: 10.1007/s10439-013-0801-y.

[13] L. C. Wu *et al.*, "In Vivo Evaluation of Wearable Head Impact Sensors," *Ann. Biomed. Eng.*, vol. 44, no. 4, pp. 1234–1245, 2016, doi: 10.1007/s10439-015-1423-3.

[14] S. Rowson *et al.*, "A six degree of freedom head acceleration measurement device for use in football," *J. Appl. Biomech.*, vol. 27, no. 1, pp. 8–14, 2011.

[15] M. A. Allison *et al.*, "Measurement of Hybrid III Head Impact Kinematics Using an Accelerometer and Gyroscope System in Ice Hockey Helmets," *Ann. Biomed. Eng.*, vol. 43, no. 8, pp. 1896–1906, 2015, doi: 10.1007/s10439-014-1197-z.

[16] L. Carey *et al.*, "Verifying Head Impacts Recorded by a Wearable Sensor using Video Footage in Rugby League: a Preliminary Study," *Sport. Med. - Open*, vol. 5, no. 1, Dec. 2019, doi: 10.1186/S40798-019-0182-3.

[17] S. Ji *et al.*, "Use of brain biomechanical models for monitoring impact exposure in contact sports," *Ann. Biomed. Eng.*, vol. 50, pp. 1389–1408, Jul. 2022, doi: 10.1007/s10439-022-02999-w.

[18] C. M. Jones *et al.*, "An Instrumented Mouthguard for Real-Time Measurement of Head Kinematics under a Large Range of Sport Specific Accelerations," 2023.

[19] A. Post *et al.*, "The effect of acceleration signal processing for head impact numeric simulations," *Sport. Eng.*, vol. 20, no. 2, pp. 111–119, 2017, doi: 10.1007/s12283-016-0219-5.

[20] A. Bailey *et al.*, "Validation of a videogrammetry technique for analysing American football helmet kinematics," *Sport. Biomech.*, vol. 19, no. 5, pp. 678–700, 2020, doi: 10.1080/14763141.2018.1513059.

[21] S. Rowson *et al.*, "Rotational Head Acceleration Measurement Techniques and Headform Characteristics: Implication on Helmet Impact Testing," *Inj. Biomech. Res. Proc. Forty First Int. Work. Rotational*, p. Abstract, 2014.

[22] Y. Liu *et al.*, "Validation and Comparison of Instrumented Mouthguards for Measuring Head Kinematics and Assessing Brain Deformation in Football Impacts," *Ann. Biomed. Eng.*, vol. 48, no. 11, pp. 2580–2598, Nov. 2020, doi: 10.1007/s10439-020-02629-3.

[23] A. Post *et al.*, "The effect of acceleration signal processing for head impact numeric simulations," *Sport. Eng.*, vol. 20, no. 2, pp. 111–119, Jun. 2017, doi: 10.1007/s12283-016-0219-5.

[24] SAE, "Society of Automotive Engineers. Instrumentation for impact Test—Part 1—Electronic instrumentation," *SAE*, 1995.

[25] F. Hernandez *et al.*, "Six Degree-of-Freedom Measurements of Human Mild Traumatic Brain Injury.," *Ann. Biomed. Eng.*, vol. 43, no. 8, pp. 1918–1934, 2015, doi: 10.1007/s10439-014-1212-4.

[26] J. M. Clark *et al.*, "Comparison of ice hockey goaltender helmets for concussion type impacts.," *Ann. Biomed. Eng.*, vol. 46, no. 7, pp. 986–1000, Jul. 2018, doi: 10.1007/s10439-018-2017-7.

[27] E. M. P. Williams *et al.*, "Sex differences in neck strength and head impact kinematics in university rugby union players," *Eur. J. Sport Sci.*, vol. 22, no. 11, pp. 1649–1658, 2022, doi: 10.1080/17461391.2021.1973573.

[28] G. Tierney *et al.*, "Head Exposure to Acceleration Database in Sport (HEADSport): a kinematic signal processing method to enable instrumented mouthguard (iMG) field-based inter-study comparisons," *BMJ Open Sport Exerc. Med.*, vol. 10, no. 1, p. e001758, Jan. 2024, doi: 10.1136/BMJSEM-2023-001758.

[29] L. Miller *et al.*, "Validation of a Custom Instrumented Retainer Form Factor for Measuring Linear and Angular Head Impact

Kinematics," *J. Biomech. Eng.*, vol. 140, no. May, pp. 1–6, 2018, doi: 10.1115/1.4039165.

[30] D. B. Camarillo *et al.*, "An instrumented mouthguard for measuring linear and angular head impact kinematics in American football.," *Ann. Biomed. Eng.*, vol. 41, no. 9, pp. 1939–49, Sep. 2013, doi: 10.1007/s10439-013-0801-y.

[31] C. Kuo *et al.*, "Effect of the mandible on mouthguard measurements of head kinematics," *J. Biomech.*, vol. 49, no. 9, pp. 1845–1853, 2016, doi: 10.1016/j.jbiomech.2016.04.017.

[32] K. Ghazi *et al.*, "American Football Helmet Effectiveness Against a Strain-Based Concussion Mechanism," *Ann. Biomed. Eng.*, vol. 50, no. 11, pp. 1498–1509, Jul. 2022, doi: 10.1007/s10439-022-03005-z.

[33] S. Wu *et al.*, "Real-time dynamic simulation for highly accurate spatiotemporal brain deformation from impact," *Comput. Methods Appl. Mech. Eng.*, vol. 394, p. 114913, May 2022, doi: 10.1016/J.CMA.2022.114913.

[34] T. B. Hoshizaki *et al.*, "The development of a threshold curve for the understanding of concussion in sport," *Trauma (United Kingdom)*, vol. 19, no. 3, pp. 196–206, Jul. 2017, doi: 10.1177/1460408616676503/ASSET/IMAGES/LARGE/10.1177_1460408616676503-FIG5.JPEG.

[35] S. Wu *et al.*, "Convolutional neural network for efficient estimation of regional brain strains," *Sci. Rep.*, vol. 9:17326, 2019, doi: https://doi.org/10.1038/s41598-019-53551-1.

[36] K. Bian and H. Mao, "Mechanisms and variances of rotation-induced brain injury: a parametric investigation between head kinematics and brain strain," *Biomech. Model. Mechanobiol.*, pp. 1–19, May 2020, doi: 10.1007/s10237-020-01341-4.

[37] S. Ji *et al.*, "Dynamic characteristics of impact-induced brain strain in the corpus callosum," *Brain Multiphysics*, vol. 3, p. 100046, 2022, doi: 10.1016/j.brain.2022.100046.

[38] C. Zhang *et al.*, "A computational pipeline towards large-scale and multiscale modeling of traumatic axonal injury," *Comput. Biol. Med.*, p. (in press), 2024, doi: https://doi.org/10.1016/j.compbiomed.2024.108109.

[39] W. Zhao and S. Ji, "Brain strain uncertainty due to shape variation in and simplification of head angular velocity profiles," *Biomech. Model. Mechanobiol.*, vol. 16, no. 2, pp. 449–461, 2017, doi: 10.1007/s10237-016-0829-7.

[40] K. El Hindi *et al.*, "Improved distance functions for instance-based text classification," *Comput. Intell. Neurosci.*, vol. 2020, 2020, doi: 10.1155/2020/4717984.

[41] D. Randall Wilson and T. R. Martinez, "Improved Heterogeneous Distance Functions," *J. Artif. Intell. Res.*, vol. 6, no. 1, pp. 1–34, 1997.

[42] S. Ji *et al.*, "Head impact accelerations for brain strain-related responses in contact sports: a model-based investigation.," *Biomech. Model. Mechanobiol.*, vol. 13, no. 5, pp. 1121–36, Oct. 2014, doi: 10.1007/s10237-014-0562-z.

[43] L. C. Wu *et al.*, "In Vivo Evaluation of Wearable Head Impact Sensors," *Ann. Biomed. Eng.*, vol. 44, no. 4, pp. 1234–1245, 2015, doi: 10.1007/s10439-015-1423-3.

[44] W. Zhao and S. Ji, "White matter anisotropy for impact simulation and response sampling in traumatic brain injury," *J. Neurotrauma*, vol. 36, no. 2, pp. 250–263, 2019, doi: 10.1089/neu.2018.5634.

[45] W. Zhao and S. Ji, "Displacement- and strain-based discrimination of head injury models across a wide range of blunt conditions," *Ann. Biomed. Eng.*, vol. 20, no. 6, pp. 1661–1677, 2020, doi: 10.1007/s10439-020-02496-y.

[46] W. Zhao *et al.*, "Displacement Error Propagation From Embedded Markers to Brain Strain," *J. Biomech. Eng.*, vol. 143, no. October, pp. 1–10, 2021, doi: 10.1115/1.4051050.

[47] S. Ji and W. Zhao, "Displacement voxelization to resolve mesh-image mismatch: application in deriving dense white matter fiber strains," *Comput. Methods Programs Biomed.*, vol. 213, p. 106528, 2022, doi: 10.1016/j.cmpb.2021.106528.

[48] N. Lin *et al.*, "A Morphologically Individualized Deep Learning Brain Injury Model," *J. Neurotrauma*, vol. 40, no. 19–20, pp. 2233–2247, Jul. 2023, doi: 10.1089/neu.2022.0413.

[49] S. Wu *et al.*, "Instantaneous brain strain estimation for automotive head impacts via deep learning," *Stapp Car Crash J.*, vol. 65, 2021.

[50] K. Ghazi *et al.*, "Instantaneous Whole-Brain Strain Estimation in Dynamic Head Impact," *J. Neurotrauma*, vol. 38, no. 8, pp. 1023–1035, 2021, doi: 10.1089/neu.2020.7281.

[51] C. Kuo *et al.*, "On-Field Deployment and Validation for Wearable Devices," *Ann. Biomed. Eng.*, vol. 50, no. 11, pp. 1372–1388, Nov. 2022, doi: 10.1007/S10439-022-03001-3/TABLES/3.

[52] S. Wu *et al.*, "Real-time dynamic simulation for highly accurate spatiotemporal brain deformation from impact," *Comput. Methods Appl. Mech. Eng.*, vol. 394, p. 114913, May 2022, doi: 10.1016/J.CMA.2022.114913.

[53] X. Zhan *et al.*, "Rapid Estimation of Entire Brain Strain Using Deep Learning Models," *IEEE Trans. Biomed. Eng.*, vol. 9294, no. c, pp. 1–11, 2021, doi: 10.1109/TBME.2021.3073380.

[54] C. Kuo *et al.*, "Comparison of video-based and sensor-based head impact exposure," *PLoS One*, vol. 13, no. 6, p. e0199238, Jun. 2018, doi: 10.1371/journal.pone.0199238.

[55] A. I. King *et al.*, "Is head injury caused by linear or angular acceleration?," in *IRCOBI Conference*, Lisbon, Portugal, Portugal, 2003, pp. 1–12.

[56] M. Fahlstedt *et al.*, "Ranking and Rating Bicycle Helmet Safety Performance in Oblique Impacts Using Eight Different Brain Injury Models," *Ann. Biomed. Eng.*, vol. 49, no. 3, pp. 1097–1109, Jan. 2021, doi: 10.1007/s10439-020-02703-w.